Structural Studies of Mycobacterium tuberculosis Rv0899 Reveal a Monomeric Membrane-Anchoring Protein with Two Separate Domains

ARTICLE *in* JOURNAL OF MOLECULAR BIOLOGY · NOVEMBER 2011

Impact Factor: 4.33 · DOI: 10.1016/j.jmb.2011.11.016 · Source: PubMed

9 AUTHORS, INCLUDING:

Chaowei Shi
Leibniz-Institut für Molekulare Pharmakolo…
19 PUBLICATIONS **116** CITATIONS
SEE PROFILE

Pan Shi
University of Science and Technology of Ch…
12 PUBLICATIONS **80** CITATIONS
SEE PROFILE

Fangming Wu
Hefei Institute of Physical Sciences, Chines…
18 PUBLICATIONS **122** CITATIONS
SEE PROFILE

Changlin Tian
University of Science and Technology of Ch…
64 PUBLICATIONS **1,236** CITATIONS
SEE PROFILE

doi:10.1016/j.jmb.2011.11.016 J. Mol. Biol. (2012) 415, 382–392

Contents lists available at www.sciencedirect.com

Journal of Molecular Biology

journal homepage: http://ees.elsevier.com.jmb

Structural Studies of *Mycobacterium tuberculosis* Rv0899 Reveal a Monomeric Membrane-Anchoring Protein with Two Separate Domains

Juan Li[1]†, Chaowei Shi[1]†, Yuan Gao[1], Kaiqi Wu[1], Pan Shi[1], Chaohua Lai[1], Liu Chen[1], Fangming Wu[2]* and Changlin Tian[1,2]*

[1]*Hefei National Laboratory for Physical Science at Microscale and School of Life Science, University of Science and Technology of China, Hefei, Anhui 230027, China*
[2]*High Magnetic Field Laboratory, Chinese Academy of Sciences, Hefei, Anhui 230031, China*

Received 12 June 2011; received in revised form 2 November 2011; accepted 8 November 2011
Available online 15 November 2011

Edited by A. G. Palmer III

Keywords:
outer membrane proteins; OmpATb; solution NMR; EPR-DEER; porin-like channel

Rv0899 from *Mycobacterium tuberculosis* belongs to the OmpA (outer membrane protein A) family of outer membrane proteins. It functions as a pore-forming protein; the deletion of this gene impairs the uptake of some water-soluble substances, such as serine, glucose, and glycerol. Rv0899 has also been shown to play a part in low-pH environment adaption, which may play a part in pathogenic mycobacteria overcoming the host's defense mechanisms. Based on many bacterial physiological data and recent structural studies, it was proposed that Rv0899 forms an oligomeric channel to carry out such functions. In this work, biochemical and structural data obtained from solution NMR and EPR spectroscopy indicated that Rv0899 is a monomeric membrane-anchoring protein with two separate domains, rather than an oligomeric pore. Using NMR chemical shift perturbation and isothermal calorimetric titration assays, we show that Rv0899 was able to interact with Zn^{2+} ions, which may indicate a role for Rv0899 in the process of Zn^{2+} acquisition.

Introduction

Mycobacterium tuberculosis is a bacterial pathogen that is responsible for the death of approximately two million people every year.[1] It is equipped with a thick and lipid-rich cell envelope, which has an extremely low permeability and provides resistance to many antibiotics.[2] The paucity of porins also contributes to the low permeability of the outer membrane of *M. tuberculosis*.[3] Among the known outer membrane proteins, Rv0899 has been reported to function as a pore-forming protein, with the properties of a porin.[1,4,5] Deletion of the *Rv0899* gene reduces the permeability of *M. tuberculosis* to several small, water-soluble substances.[1] Rv0899 also contributes to the self-defense mechanism of *M. tuberculosis* in low-pH environments[1,6] through a mechanism that accelerates ammonia secretion.[7] Rv0899 is composed of three domains: an M domain that contains a transmembrane helix, a B domain

**Corresponding authors.* F. Wu is to be contacted at High Magnetic Field Laboratory, Chinese Academy of Sciences, 350 Shushanhu Road, Hefei, Anhui 230031, China; C. Tian, School of Life Science, University of Science and Technology of China, 443 Huangshan Road, Hefei, Anhui 230027, China. E-mail addresses: fmwu@hmfl.ac.cn; cltian@ustc.edu.cn.

† J.L. and C.S. contributed equally to this work.

Abbreviations used: LDAO, lauryldimethylamine oxide; TROSY, transverse relaxation optimized spectroscopy; HSQC, heteronuclear single quantum coherence; NOE, nuclear Overhauser enhancement; MTSL, (1-oxyl-2,2,5,5-tetramethyl-Δ3-pyrroline-3-methyl) methanethiosulfonate; PRE, paramagnetic relaxation enhancement; DEER, double electron–electron resonance; OmpA, outer membrane protein A; ITC, isothermal titration calorimetry; PDB, Protein Data Bank; 3D, three-dimensional.

that shares homology with BON[8] (bacterial OsmY and nodulation), and a C domain that shows high level of similarity with *Escherichia coli* OmpA[9] (outer membrane protein A). It has been shown that the pore-forming properties of Rv0899 mainly depend on the M and B domains.[6] Recently, the NMR solution structures of the B domain (residues 73–204)[10,11] and the C domain (residues 198–326)[10] were independently determined by two different groups. Interestingly, these two groups proposed two entirely different models, continuing the controversy over the pore-forming ability of Rv0899.[10,11] Structural studies of the intact protein (residues 1–326) and a truncated form (residues 52–326) of Rv0899 were conducted to address this problem. Analysis of the protein solubility and lipid interactions showed that the M domain is required for Rv0899 to integrate into the membrane, while the B+C domains were soluble and pure-monomer proteins and did not show any interaction with the lipid bilayer. Using solution NMR and EPR spectroscopy, the structure of the soluble region of Rv0899 (residues 75–326) was determined to be monomeric and to contain two separate domains (B and C domains). Working from our results, we proposed that it is impossible for Rv0899 to form a channel through the oligomerization of its M domain and/or B domain. A structural homologous comparison—as well as an analysis of the interaction between $Rv0899_{52–326}$ and the peptidoglycan components—provided some hints on the possible location and orientation of Rv0899 in the mycobacterial membrane. Further chemical shift perturbation and isothermal titration calorimetry (ITC) assays showed that Rv0899 was able to bind to zinc ions, which indicated that Rv0899 may play a role in Zn^{2+} acquisition.

Results and Discussion

Rv0899 was anchored in the membrane through its N-terminus (residues 1–51), while the B and C domains were distant from the lipid bilayer

A sequence of 23 hydrophobic amino acids (residues 28–50) was predicted to form a transmembrane helix (using TMHMM Server v.2.0‡). The N-terminal M domain (including the predicted hydrophobic helix) has been reported to be essential, due to its membrane translocation and pore-forming activity.[4] Therefore, a truncated form of Rv0899 (residues 52–326), as well as the intact protein (residues 1–326), was overexpressed and purified for biochemical and structural studies. $Rv0899_{1–326}$ was expressed in the *E. coli* membrane fraction and could be solubilized in various detergents, such as lauryldimethylamine oxide (LDAO); however, it precipitated in aqueous buffer, as shown in the SDS-PAGE results of ultracentrifugation analysis (Supplementary Fig. S1). In contrast, $Rv0899_{52–326}$ was expressed as a water-soluble protein. Size-exclusion chromatography of $Rv0899_{52–326}$ showed a monomeric protein in aqueous solution (Supplementary Fig. S2), which was consistent with the recent report of Teriete *et al.*[11] This was further verified by the negative liposome reconstitution result from $Rv0899_{52–326}$ in DMPC/DMPG (dimyristoylphosphatidylcholine/dimyristoylphosphatidylglycerol) (Supplementary Fig. S3). Furthermore, Rv0899 of *M. tuberculosis* had already been proven to be an integral membrane protein rather than a peripheral membrane protein,[12] using a method that can differentiate integral membrane protein from peripheral membrane protein.[13,14] Therefore, it could be concluded that Rv0899 was anchored to the membrane with its M domain transmembrane helix region (residues 28–50).

$^{1}H–^{15}N$ transverse relaxation optimized spectroscopy (TROSY)-heteronuclear single quantum coherence (HSQC) spectra were recorded for the two polypeptides ($Rv0899_{1–326}$ and $Rv0899_{52–326}$) to analyze the interactions between the Rv0899 domains and the lipid bilayer. Surprisingly, the HSQC spectrum for $Rv0899_{1–326}$ in LDAO was quite similar to that of $Rv0899_{52–326}$ in aqueous buffer, except for some extra resonances coming from the residues of M domain (Fig. 1). This result indicated that the conformation of the soluble region of Rv0899 (B+C domains, residues 52–326) was similar in these two polypeptides, and there was no direct interaction between the B+C domains of Rv0899 and the detergent micelles. It was therefore possible to conclude that the M domain was essential for the integration of Rv0899 in the lipid bilayer, while the soluble region of Rv0899 (B+C domains, residues 52–326) was kept away from the lipid bilayer. In addition, the resonance linewidths for the intact protein ($Rv0899_{1–326}$) in LDAO micelles were observed to be similar to those of $Rv0899_{52–326}$, indicating that $Rv0899_{1–326}$ did not form an oligomer, even in the presence of the M domain and the detergent micelles.

Structure determination of $Rv0899_{75–326}$ using solution NMR and EPR spectroscopy

The solution structures of the B domain (residues 79–195) and C domain (residues 208–326) of Rv0899 were separately determined by two independent groups.[10,11] However, the structure of Rv0899 containing both the B and C domains has not yet been reported since they were thought to be connected by a flexible linker.[11] Here, a backbone

‡http://www.cbs.dtu.dk/services/TMHMM/

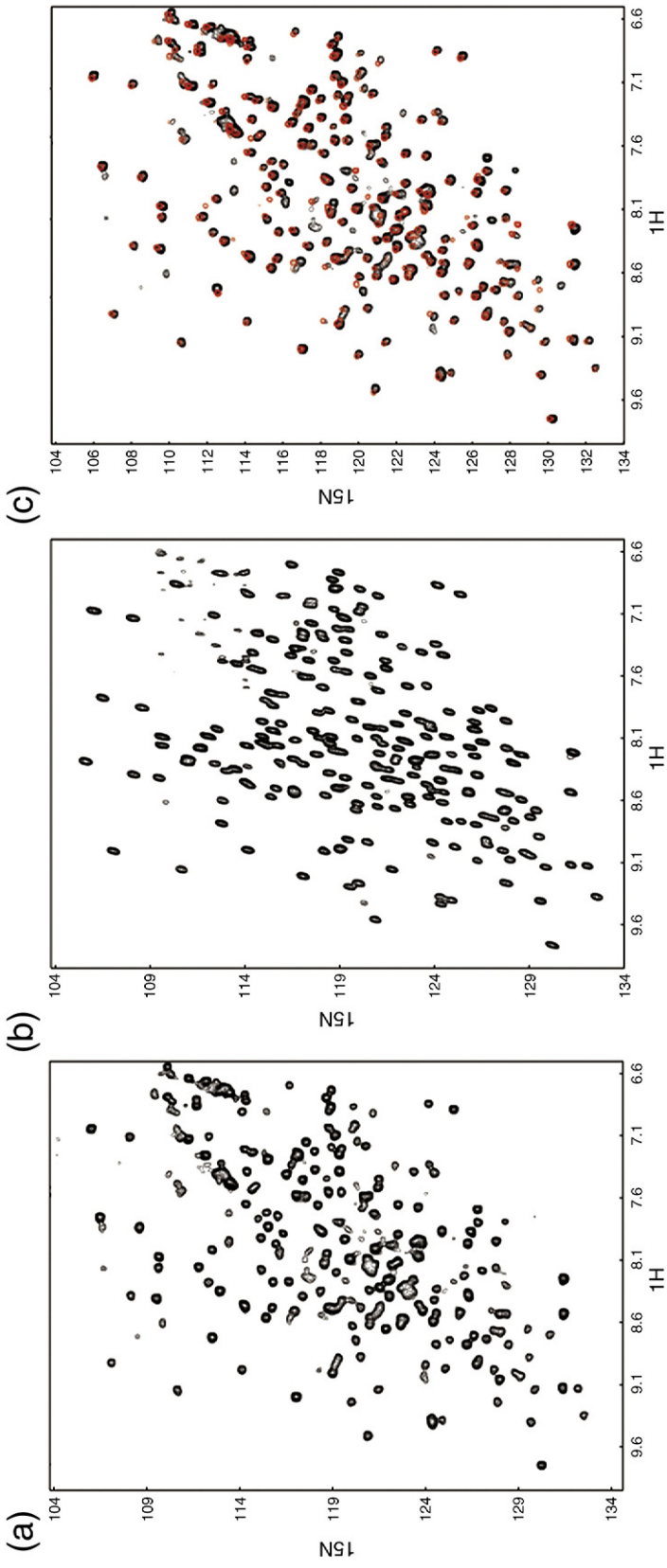

Fig. 1. The TROSY-HSQC spectra for $Rv0899_{1–326}$ in LDAO (a) and $Rv0899_{52–326}$ in aqueous buffer (b). The two spectra are shown to overlay closely in (c) (black, $Rv0899_{1–326}$; red, $Rv0899_{52–326}$).

amide ^{15}N relaxation analysis of $Rv0899_{52–326}$ showed uniform levels of T_1, T_2, and heteronuclear $^{1}H–^{15}N$ nuclear Overhauser enhancement (NOE), strongly indicating a coherent dynamic along the primary sequence of the protein (Fig. 2). This provided the motivation to attempt a determination of the relative orientation of these two domains. Unfortunately, although 2054 NOE restraints were obtained, none of them was assigned between the two protons coming from the B and C domains (one proton from each domain). To obtain information on the two domains' relative orientation, we applied paramagnetic relaxation enhancement (PRE) and

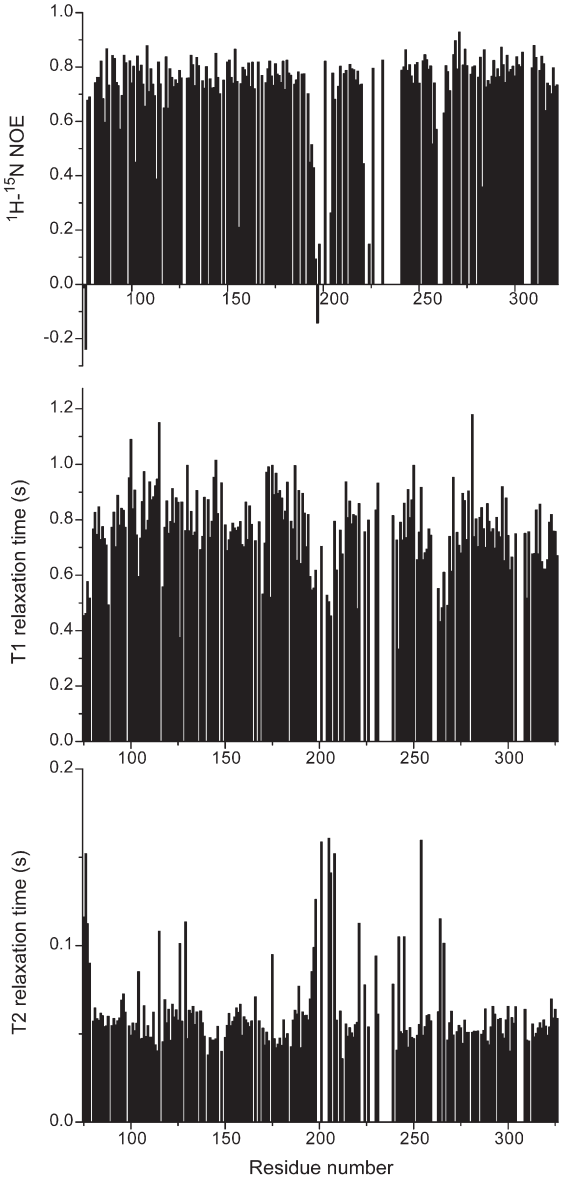

Fig. 2. Backbone amide ^{15}N relaxation analysis of $Rv0899_{52–326}$ ($^{1}H–^{15}N$ heteronuclear NOE, T_1 relaxation, and T_2 relaxation).

EPR spectroscopies to collect long-distance restraints. According to the structure of the C domain [Protein Data Bank (PDB) IDs: 2KGW[10] and 2L26], a disulfide bond was formed between the only two cysteines (Cys208 and Cys250) in the original sequence of Rv0899. Therefore, these two cysteines were retained, as they will not impact specific spin labeling. Four residues (Gly117 and Ser136 in the B domain, and Thr256 and Ser302 in the C domain) were then respectively mutated to cysteine for subsequent spin radical (1-oxyl-2,2,5,5-tetramethyl-Δ3-pyrroline-3-methyl) methanethiosulfonate (MTSL) labeling. Alternatively, the spin radicals could be reduced with the addition of ascorbic acid to obtain the diamagnetic reference spectrum. The intensity attenuations of the HSQC amide proton resonances were analyzed by comparing the paramagnetic and diamagnetic spectra. The collected signal intensity attenuations were used to calculate the distance between the observed amide proton and the MTSL nitrogen atom, according to the Solomon–Bloembergen equation;[15] 428 long-distance restraints were obtained from the PRE measurements, and these restraints were used in the structure calculations.

DEER (double electron–electron resonance) can provide quantitative long-distance information between two spin labels. To prepare the protein sample for DEER spectroscopy, three pairs of residues (Gly117/Ser302, G117/Thr256, and Ser136/Thr256) were mutated by cysteines and then labeled by MTSL. The distances of these three cysteine pairs were then obtained, based on the DEER spectra and subsequent data analysis. The restraints derived from PRE, EPR, and solution NMR (such as NOE, hydrogen bond, and dihedral angle) were used to calculate the structure of $Rv0899_{52–326}$. The 10 lowest-energy structures were selected out of the 100 accepted structures. Information on the restraints used in the structure calculation and statistics about the quality and precision of the structures are summarized in Table 1. The final structures were converged with two separate domains, which were maintained in a rigid relative domain–domain orientation (Fig. 3). This well-defined orientation between the two separate domains has also been found in other bacterial outer membrane proteins, such as the tandem POTRA domains of BamA from *E. coli*.[16]

The resulting $Rv0899_{52–326}$ structure was compared to previously reported single-domain structures[10,11] using SSM software (v.2.36).[17] It was noted that the three B-domain structures derived by three independent research groups were quite similar; the B-domain structure comprises two layers: one β-strand layer and one α-helix layer (Supplementary Fig. S4a). In contrast, the C-domain structures reported by us and Yang *et al.*[10] showed some small differences (Supplementary Fig. S4b).

Table 1. Summary of structural statistics for the 10 final structures of $Rv0899_{52–326}$

Conformationally restricting constraints	2873
NOE distance constraints	
Intraresidue ($i=j$)	645
Sequential ($\|i-j\|=1$)	785
Medium range ($1<\|i-j\|<5$)	279
Long range ($\|i-j\|\geq 5$)	345
Hydrogen bond constraints	88
Dihedral angle constraints	300
PRE constraints	428
DEER constraints	3
Average pairwise backbone rmsd (Å)	
B domain (79–195)	0.729
C domain (208–220, 240–326)	1.435
B and C domains	2.434
Whole length (75–326)	3.003
Ramachandran plot statistics (%)	
Most favored regions	77.9
Additional allowed regions	16.7
Generously allowed	4.1
Disallowed regions	1.3

Average pairwise backbone rmsd (Å) with different pair restraints

Constraint seeds	Whole length	B domain	C domain	B+C domains
NOE	10.258	0.978	1.452	9.358
NOE, PRE	4.203	0.717	1.470	3.748
NOE, DEER	7.867	1.047	1.797	7.050
NOE, PRE, DEER	3.003	0.729	1.435	2.434

Rv0899 is a membrane-anchoring protein, but not a porin

For a long time, Rv0899 has been considered as a pore-forming protein with a β-barrel conformation, similar to *E. coli* OmpA. Only one transmembrane helix (residues 28–50) was predicted to be present in the N-terminal M domain of Rv0899.[4] Here, the CD spectrum of $Rv0899_{1–73}$ in LDAO consistently indicated that this region had an α-helix content of around 30% in its secondary structure (Supplementary Fig. S5). It would be impossible for this region to form a pore (via the oligomerization of this hydrophobic helix segment of the M domain) that allowed the diffusion of small hydrophilic molecules, since it lacks all of the hydrophilic residues (which are needed to line up a pore surface) from the predicted transmembrane helix, except Arg29. Furthermore, $Rv0899_{52–326}$ is a pure monomer in both LDAO and aqueous buffer (Supplementary Fig. S1). We can therefore also exclude the possibility that Rv0899 forms a pore through the oligomerization of its C-terminal region (B and C domains), although this strategy is adopted by MotB from *Salmonella typhimurium*.[18]

According to the conclusively determined monomeric properties and NMR structure of $Rv0899_{52–326}$, we propose that Rv0899 is a membrane-anchoring protein, but not a porin. Recent *in vivo* functional studies have consistently indicated that Rv0899 (OmpATb) lacks porin activity in both *M. tuberculosis* and *Mycobacterium smegmatis*.[7]

The organization of Rv0899 in the cell envelope of *M. tuberculosis*

Many biochemical studies, such as the proteinase K cleavage assay by Song *et al.*,[19] have provided solid evidence that Rv0899 is located in the outer membrane of *M. tuberculosis*. Since we have excluded the possibility that Rv0899 acts as a pore-forming channel, what is this mysterious protein's function and organization in the outer membrane? We note that the C domain of Rv0899 is a putative peptidoglycan-binding domain, since its primary sequence and three-dimensional (3D) structure share many similarities with several cell-wall-interacting proteins, such as OmpA,[9] MotB,[18] RmpM,[20] and PAL[21] (Fig. 4). Nevertheless, the possibility of interaction between the water-soluble region (residues 52–326) of Rv0899 and the periplasmic region of *M. tuberculosis* was excluded, as the binding assays of $Rv0899_{52–326}$ with peptidoglycan components [NAM (*N*-acetylmuramic acid) and NAG (*N*-acetylglucosamine)] were negative (Supplementary Fig. S6a and b). Furthermore, $Rv0899_{52–326}$ failed to bind mannose and glucose (Supplementary Fig. S6c and d), suggesting that there should be no specific interaction between Rv0899 and the polysaccharide-rich capsule envelope of *M. tuberculosis*. We therefore believe that Rv0899 anchors to the outer membrane with its N-terminal region (M domain), while the C-terminal region (B and C domains) extrudes to the extracellular side of *M. tuberculosis*. Teriete *et al.* proposed four possible model arrangements of the

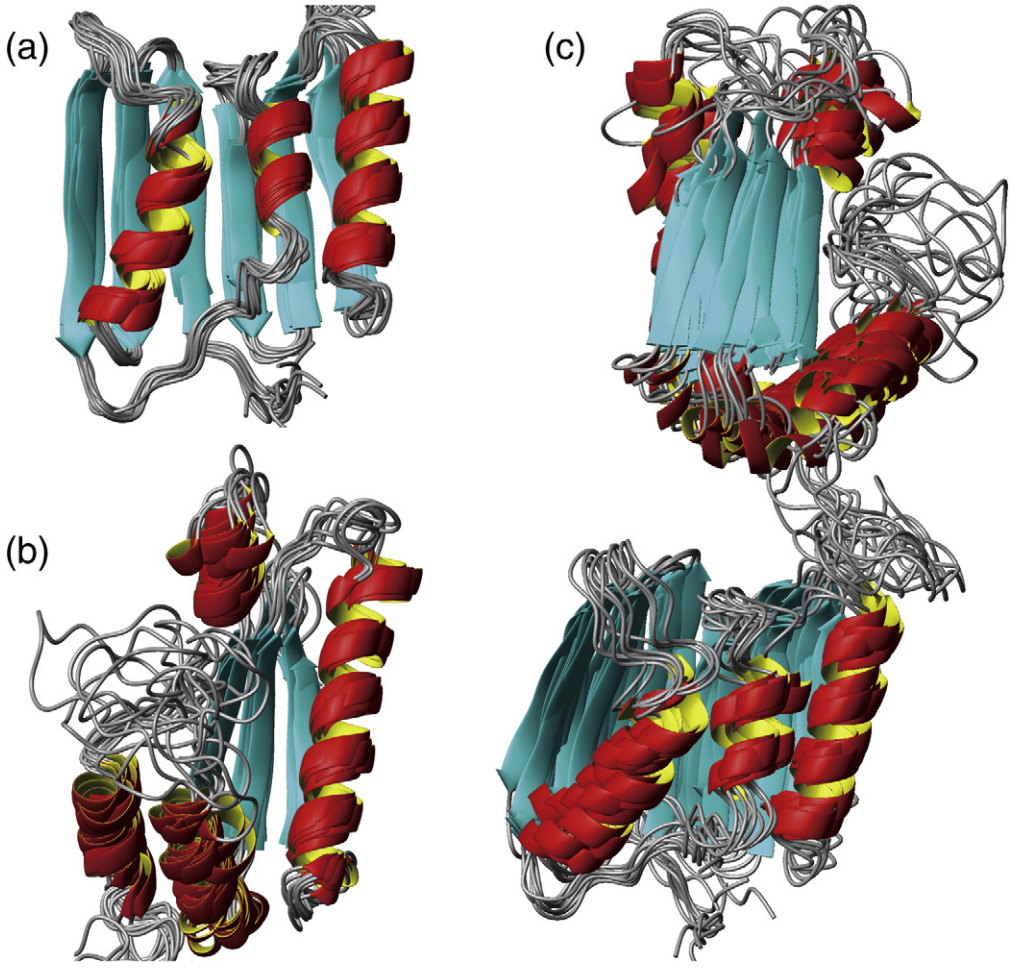

Fig. 3. Ribbon presentation of the solution structure of the B domain (a), C domain (b), and B + C domains (c) of Rv0899. B domain, residues 79–195; C domain, residues 208–326; B + C domain, residues 75–326. The final 10 conformers with the lowest energies are superimposed in this figure.

protein within the mycobacterial envelope,[11] and we show here that their first model is consistent with our results (Fig. 5).

A putative function of Rv0899 in zinc ion acquisition

Since the above results contradict the long-accepted channel conformation of Rv0899, what is the possible function of this membrane protein? To answer this question, we tried to screen Rv0899's interaction partner using ITC. Various hydrophilic compounds, such as glucose, mannose, serine, Zn^{2+}, and Cu^{2+}, were used in this screening. Most of them failed to interact with Rv0899 (Supplementary Fig. S6c and d), but Zn^{2+} ions showed positive results in the ITC assay (Fig. 6a) and the NMR titration experiment using $Rv0899_{52–326}$ (Figs. 6b and 7a). Saturable binding curves were observed, and the dissociation constant (K_d) was derived to be around 0.1–0.2 mM by fitting the data obtained from these two methods (Fig. 6 and Table 2). Resonances (whose chemical shift values were obviously perturbed upon the binding of Zn^{2+}) were assigned and mapped to the structure of Rv0899 (Fig. 7b). The putative zinc binding site turned out to be close to the N-terminal region of the B domain (Fig. 7b). It is well known that zinc ions are essential in DNA replication and transcription activities and that uptake of zinc ions is normally tightly regulated. However, the mechanism of Zn^{2+} uptake has not been well studied in *M. tuberculosis*. Although it is impossible for Rv0899 to import Zn^{2+} directly across the outer membrane, it may play some essential role in enriching Zn^{2+} ions for further acquisition. It has been reported that the deletion of the *Rv0899* gene reduces the permeability to several small water-soluble substances.[1] Considering these two phenomena together, we propose the possibility that there is a protein complex that functions in the acquisition of zinc ions (and/or other nutrients); Rv0899 may play an assistant role in recruiting Zn^{2+}

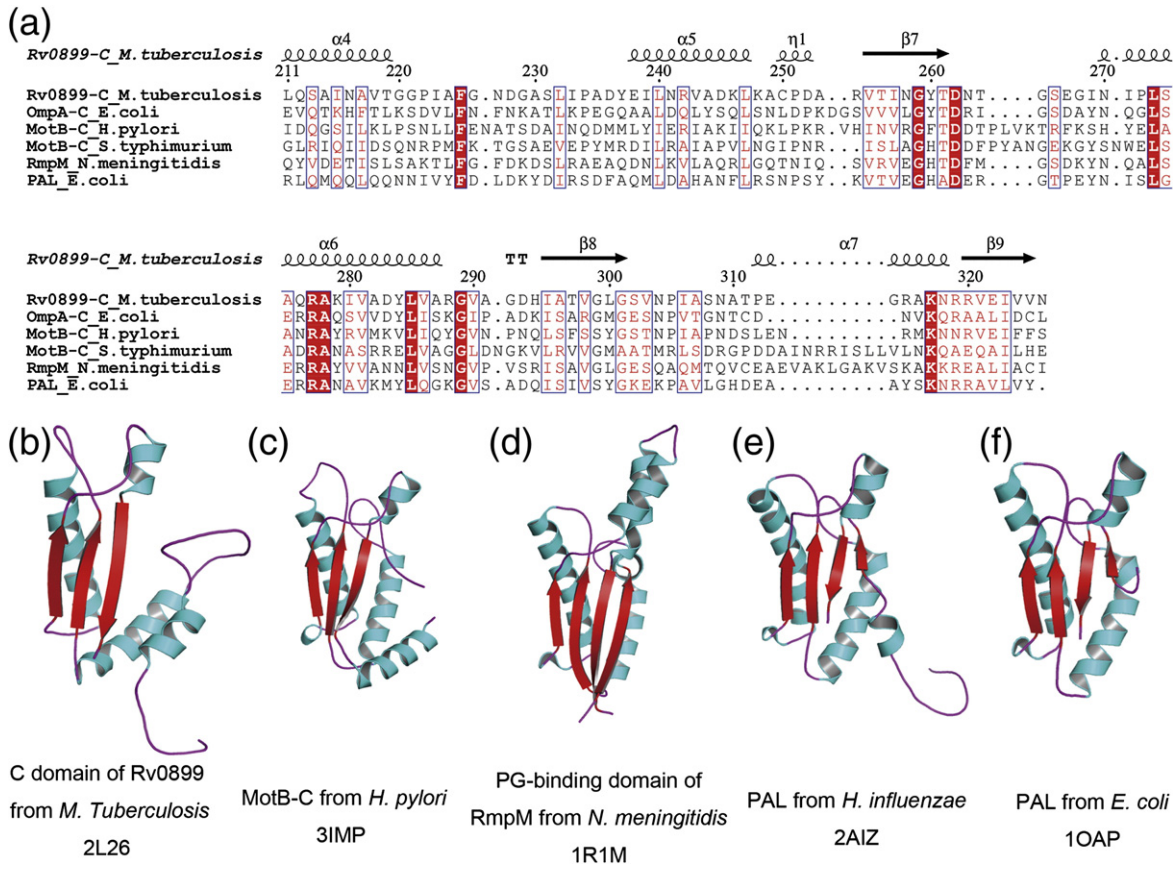

Fig. 4. (a) Sequence alignment of OmpA-like domains from different species. 3D structure comparison of Rv0899 C domain (b), MotB-C from *Helicobacter pylori* (c), the PG binding domain of RmpM from *Neisseria meningitidis* (d), and the periplasmic domains of PALs from *Haemophilus influenzae* (e) and *E. coli* (f). The PDB accession codes are listed below each structure.

ions into the periphery of *M. tuberculosis*, and there may be another protein acting to form pores, providing a path for small water-soluble substances. Certainly, further studies are required to validate this hypothesis and to provide an understanding of this mechanism.

Materials and Methods

Protein expression and purification of $Rv0899_{1–326}$ and $Rv0899_{52–326}$

The gene fragments encoding $Rv0899_{1–326}$ and $Rv0899_{52–326}$ were PCR amplified from the *M. tuberculosis* DNA library and then inserted into pET-21a vector (Novagen) with a C-terminal 6× His tag. The recombinant protein was expressed in *E. coli* BL21(DE3) cells in M9 media and induced with 0.8 mM IPTG at 37 °C for 5 h. The isotopically enriched proteins were prepared using 1 g/L $^{15}NH_4Cl$ as the sole nitrogen source and 3 g/L $^{2}H,^{13}C$-glucose (Cambridge Isotope Laboratories, Andover, MA) as the sole carbon source. The proteins were purified using Ni-NTA resin (QIAgen, Valencia, CA) and subsequent size-exclusion chromatography (HiLoad 16/60 Superdex 75 10/300, GE Healthcare). The detergent LDAO was used in the purification process. The final NMR buffer was 50 mM NaH_2PO_4/Na_2HPO_4 and 0.2% LDAO, pH 7.2.

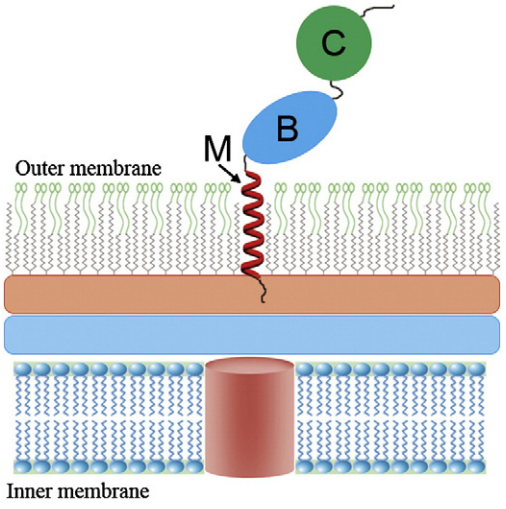

Fig. 5. A possible model for the organization of Rv0899 in the *M. tuberculosis* membrane, consistent with the first model proposed by Teriete *et al.*[11]

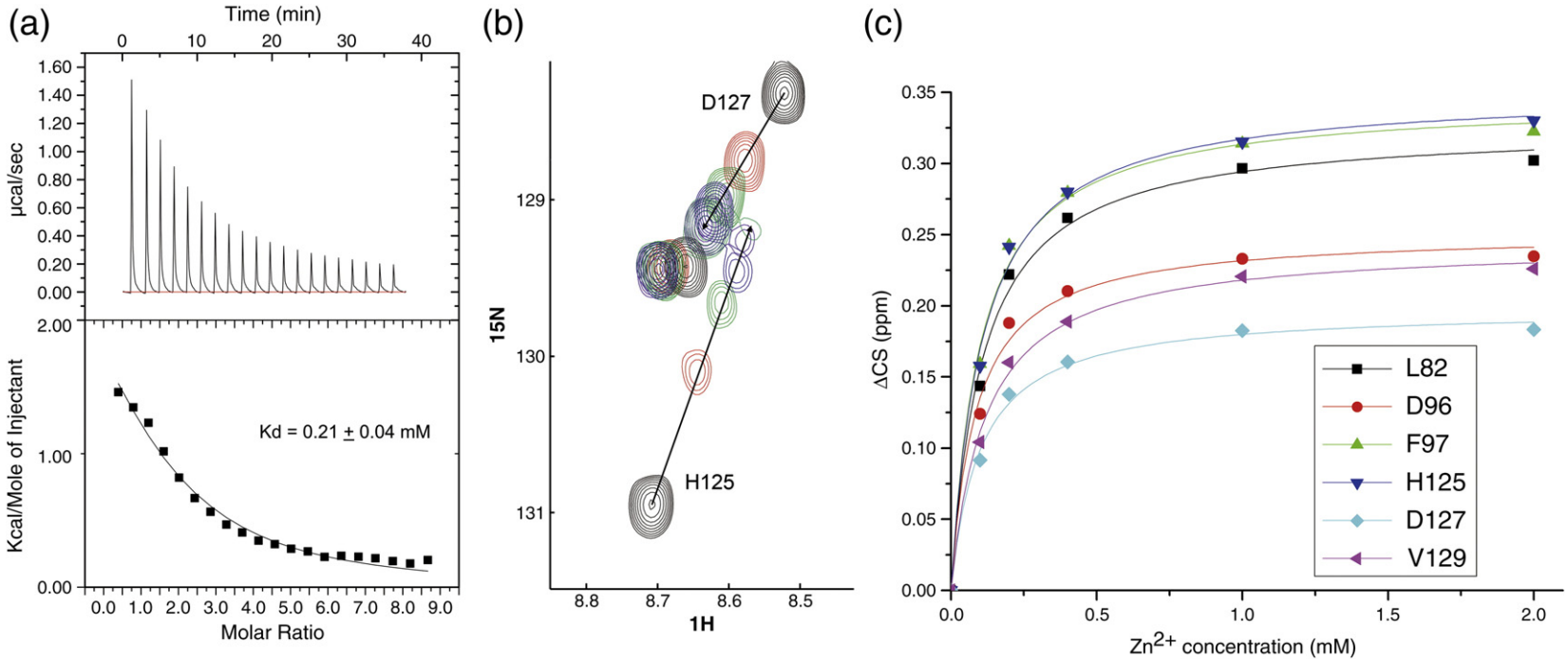

Fig. 6. Binding assays between $Rv0899_{52–326}$ and zinc ions. (a) Original data (upper panel) and fitting curve (lower panel) from the ITC experiment. (b) Shifts in the peaks of two representative residues that were obviously perturbed in the NMR titration experiment. (c) Curves fitted to the chemical shift data (using Origin 8.0).

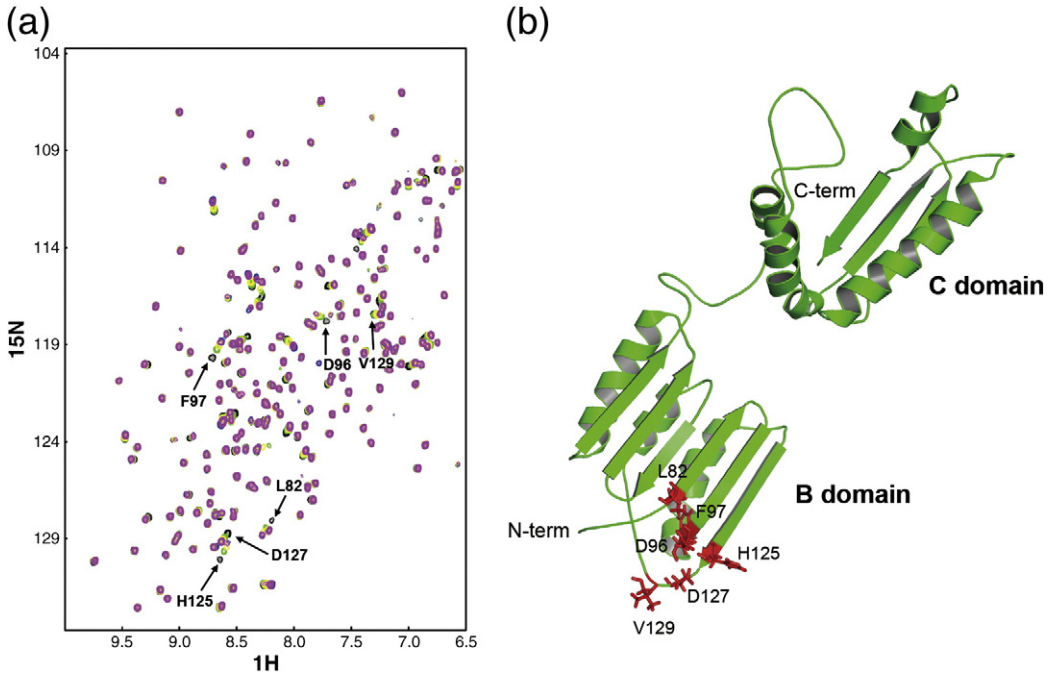

Fig. 7. Solution NMR chemical shift perturbation assay showing the binding interface between Zn^{2+} and $Rv0899_{52–326}$. (a) NMR HSQC spectra overlapping for $Rv0899_{52–326}$ in the presence of different concentrations of Zn^{2+} ions (Zn^{2+}/$Rv0899_{52–326}$ molar ratios: 0.5, 1.0, 2.0, 5.0, and 10.0). Residues with pronounced chemical shift changes are annotated. (b) Location of residues in the $Rv0899_{52–326}$ structure that showed chemical shift perturbation with the introduction of Zn^{2+} ions.

$Rv0899_{52–326}$ expression and purification for titration experiments

The $Rv0899_{52–326}$ DNA fragment was cloned into the pET-21a vector without 6 × His tag. The protein was purified using DEAE (diethylaminoethyl) Sepharose, HiTrapQ Sepharose XL, and size-exclusion chromatography (Superdex 75, 10/300). The ^{15}N-labeled sample was concentrated to a final concentration of 0.6–0.8 mM for NMR titration. The unlabeled protein was concentrated to 0.1 mM for ITC.

Protein expression and purification for spin labeled $Rv0899_{52–326}$

Mutations were carried out using PCR site-directed mutagenesis for G117C, S136C, T256C, or S302C. The expression and purification of ^{15}N-labeled $Rv0899_{52–326}$ mutant were similar to the wild type. Spin radical probe MTSL (Toronto Research Chemicals) was introduced to the specific site through disulfide bond formation between MTSL and the cysteine of the protein. The reaction between the MTSL and cysteine residues was conducted in reaction buffer (20 mM Tris and 200 mM NaCl, pH 8.0), at 37 °C for 4 h. Free and redundant MTSL was removed through ultracentrifugation and size-exclusion chromatography.

Ultracentrifugation analysis and liposome reconstitution experiment

Ultracentrifugation experiment was employed to prove that $Rv0899_{1–326}$ was expressed in *E. coli* membrane. The cells expressing $Rv0899_{1–326}$ were sonicated and low speed centrifuged at 16,000 rpm for 20 min at 4 °C (HITACHI centrifuge, himac CR2IGII) to remove insolubles (such as cell debris, inclusion bodies, etc.). The resulting supernatant fraction, which included the soluble fraction and membrane fraction, was further processed by ultracentrifugation (150,000*g*, 2 h) to obtain the membrane fraction (Beckman Coulter, optimaTM L-100XP). Then, the composition of the membrane fraction was analyzed by SDS-PAGE.

DMPC/DMPG liposomes were prepared with a molar ratio of 4:1. Then, the liposomes were added to the protein solution with a lipid:protein ratio of 200:1. The protein solution was dialyzed against 50 mM Na_2HPO_4/NaH_2PO_4, pH 8.0, with the buffer changed three times, and then dialyzed against 50 mM Na_2HPO_4/NaH_2PO_4, pH 6.5, with two more buffer changes. The dialyzed solution was ultracentrifuged (150,000*g*, 2 h, Beckman Coulter, optimaTM L-100XP) and analyzed by SDS-PAGE.

Table 2. The obtained K_d values determined by fitting the NMR chemical shift perturbation data to a single-site ligand-binding model (Origin)

Residue	K_d (mM)
L82	0.11 ± 0.01
D96	0.09 ± 0.01
F97	0.10 ± 0.01
H125	0.11 ± 0.01
D127	0.10 ± 0.01
V129	0.12 ± 0.01

NMR/PRE/EPR spectroscopy and structure determination

A set of TROSY-based triple-resonance, multi-dimensional NMR experiments were conducted for $^{13}C/^{15}N$ $Rv0899_{52–326}$ in 50 mM Na_2HPO_4/NaH_2PO_4, pH 6.5, at 30 °C, on a 600-MHz Bruker spectrometer. The NMR experiments included HNCO, HN(CA)CO, HNCACB, and HN(CO)CACB. 3D $^{15}N/^{1}H$ NOESY (NOE spectroscopy)-HSQC and a $^{13}C/^{1}H$ NOESY-HSQC were also acquired to collect NOE restraints. All the data were processed using NMRPipe,[22] with both forward and backward linear prediction to improve the resolution in each indirect dimension. The resulting NMR spectra were analyzed using NMRView[23] for backbone assignment and Sparky for NOE assignment.

$[^{1}H–^{15}N]$-TROSY-HSQC spectra of MTSL-labeled $Rv0899_{52–326}$ were acquired. The same two-dimensional spectra were repeated, after the spin radicals were reduced with the addition of two- to threefold excess ascorbic acid. Samples were placed in the magnet at 30 °C for at least 30 min before data acquisition, to ensure complete reduction of the spin radicals.

DEER spectra of $Rv0899_{52–326}$ with double MTSL labeling were acquired at 66 K on a pulsed EPR spectrometer E580 (Bruker Biospin, Switzerland). Data were analyzed using DeerAnalysis2006 software.[24] In DEER data processing, background echo decay signals were corrected using a homogeneous 3D spin distribution. After data were Fourier transformed, the best-fit Pake pattern was obtained through optimizing the starting time for the background fit and the lowest rmsd background fit. The Pake pattern and the equation below were applied to determine the distance between two radicals:

$$f_{\mathrm{Dip}}(r,\theta) = \frac{\mu_B^2 g_A g_B \mu_0}{2\pi h} \cdot \frac{1}{r_{AB}^3}\left(3\cos^2\theta - 1\right)$$

where θ is the angle between the spin–spin vector r and the direction of the applied magnetic field, μ_B is the Bohr magneton, μ_0 is the permeability of free space, g_A and g_B are the g values for the two spin labels A and B, and r is the spin–spin distance, assuming the exchange coupling constant can be neglected. A mean distance can be inferred once a resolved perpendicular turning point feature is observed in the spectrum.

Backbone torsion angle restraints were predicted from assigned backbone chemical shifts (^{13}CO, $^{13}C^{\alpha}$ and $^{13}C^{\beta}$), using the TALOS+ program.[25] The backbone dihedral angle, NOE, and long-distance restraints from PRE and EPR were used in the structure calculations for $Rv0899_{52–326}$, using the program Xplor-NIH.[26] The final 10 structures with the lowest energy were verified using PROCHECK-NMR software.[27]

ITC assay and NMR titration experiments

ITC experiments were performed using an iTC_{200} microcalorimeter (MicroCal) in ITC buffer (25 mM Hepes and 100 mM NaCl, pH 6.5) at 30 °C. $ZnSO_4$ or other hydrophilic compounds were dissolved in ITC buffer and adjusted to pH 6.5 and then used directly in titration experiments. Both the protein sample and ligand solution were degassed extensively, and their concentrations were determined precisely using absorption spectrometers. Twenty injections of $ZnSO_4$ stock (4 mM) into the calorimeter cell, which was completely filled with protein solution (0.1 mM), were collected at 120-s intervals. The data were analyzed and plotted using MicroCal Origin software.

The binding locations of Zn^{2+} on $Rv0899_{52–326}$ were further analyzed using solution NMR titration. $[^{1}H–^{15}N]$-TROSY-HSQC spectra of 1.0 mM $Rv0899_{52–326}$ (without 6 × His tag) were acquired in the absence or presence of different concentrations of Zn^{2+} ions (0.5 mM, 1.0 mM, 2.0 mM, 5.0 mM, and 10.0 mM).

Data bank accession numbers

Coordinates for the structure of $Rv0899_{75–326}$ have been deposited in the PDB (accession code: 2L26). NMR assignments have been deposited in the Biological Magnetic Resonance Bank (accession number: 17863).

Acknowledgements

The authors are grateful for the Rv0899 DNA from Dr. B. Sun of the University of Science and Technology of China. We also thank Dr. F. M. Marassi of the Sanford Burnham Institute, La Jolla, CA, and Dr. M. Niederweis of the University of Alabama, Birmingham, AL, for great discussions and suggestions. This study was supported by the Chinese Key Research Plan (No. 2011CB911104) and Chinese National High-Tech Research Grant (No. 2006AA02A321).

Supplementary Data

Supplementary data associated with this article can be found, in the online version, at doi:10.1016/j.jmb.2011.11.016

References

1. Raynaud, C., Papavinasasundaram, K. G., Speight, R. A., Springer, B., Sander, P., Bottger, E. C. *et al.* (2002). The functions of OmpATb, a pore-forming protein of *Mycobacterium tuberculosis*. *Mol. Microbiol.* **46**, 191–201.
2. Niederweis, M. (2008). Nutrient acquisition by mycobacteria. *Microbiology*, **154**, 679–692.
3. Niederweis, M. (2003). Mycobacterial porins—new channel proteins in unique outer membranes. *Mol. Microbiol.* **49**, 1167–1177.
4. Alahari, A., Saint, N., Campagna, S., Molle, V., Molle, G. & Kremer, L. (2007). The N-terminal domain of OmpATb is required for membrane translocation and pore-forming activity in mycobacteria. *J. Bacteriol.* **189**, 6351–6358.

5. Senaratne, R. H., Mobasheri, H., Papavinasasundaram, K. G., Jenner, P., Lea, E. J. & Draper, P. (1998). Expression of a gene for a porin-like protein of the OmpA family from *Mycobacterium tuberculosis* H37Rv. *J. Bacteriol.* **180**, 3541–3547.
6. Molle, V., Saint, N., Campagna, S., Kremer, L., Lea, E., Draper, P. & Molle, G. (2006). pH-dependent pore-forming activity of OmpATb from *Mycobacterium tuberculosis* and characterization of the channel by peptidic dissection. *Mol. Microbiol.* **61**, 826–837.
7. Song, H., Huff, J., Janik, K., Walter, K., Keller, C., Ehlers, S. *et al.* (2011). Expression of the ompATb operon accelerates ammonia secretion and adaptation of *Mycobacterium tuberculosis* to acidic environments. *Mol. Microbiol.* **80**, 900–918.
8. Yeats, C. & Bateman, A. (2003). The BON domain: a putative membrane-binding domain. *Trends Biochem. Sci.* **28**, 352–355.
9. Pautsch, A. & Schulz, G. E. (2000). High-resolution structure of the OmpA membrane domain. *J. Mol. Biol.* **298**, 273–282.
10. Yang, Y., Auguin, D., Delbecq, S., Dumas, E., Molle, G., Molle, V. *et al.* (2011). Structure of the *Mycobacterium tuberculosis* OmpATb protein: a model of an oligomeric channel in the mycobacterial cell wall. *Proteins*, **79**, 645–661.
11. Teriete, P., Yao, Y., Kolodzik, A., Yu, J., Song, H., Niederweis, M. & Marassi, F. M. (2010). *Mycobacterium tuberculosis* Rv0899 adopts a mixed alpha/beta-structure and does not form a transmembrane beta-barrel. *Biochemistry*, **49**, 2768–2777.
12. Xiong, Y., Chalmers, M. J., Gao, F. P., Cross, T. A. & Marshall, A. G. (2005). Identification of *Mycobacterium tuberculosis* H37Rv integral membrane proteins by one-dimensional gel electrophoresis and liquid chromatography electrospray ionization tandem mass spectrometry. *J. Proteome Res.* **4**, 855–861.
13. YaDeau, J. T., Klein, C. & Blobel, G. (1991). Yeast signal peptidase contains a glycoprotein and the Sec11 gene product. *Proc. Natl Acad. Sci. USA*, **88**, 517–521.
14. Whitelegge, J. P., le Coutre, J., Lee, J. C., Engel, C. K., Prive, G. G., Faull, K. F. & Kaback, H. R. (1999). Toward the bilayer proteome, electrospray ionization-mass spectrometry of large, intact transmembrane proteins. *Proc. Natl Acad. Sci. USA*, **96**, 10695–10698.
15. Clore, G. M. & Iwahara, J. (2009). Theory, practice, and applications of paramagnetic relaxation enhancement for the characterization of transient low-population states of biological macromolecules and their complexes. *Chem. Rev.* **109**, 4108–4139.
16. Ward, R., Zoltner, M., Beer, L., El Mkami, H., Henderson, I. R., Palmer, T. & Norman, D. G. (2009). The orientation of a tandem POTRA domain pair, of the beta-barrel assembly protein BamA, determined by PELDOR spectroscopy. *Structure*, **17**, 1187–1194.
17. Krissinel, E. & Henrick, K. (2004). Secondary-structure matching (SSM), a new tool for fast protein structure alignment in three dimensions. *Acta Crystallogr., Sect. D: Biol. Crystallogr.* **60**, 2256–2268.
18. Kojima, S., Imada, K., Sakuma, M., Sudo, Y., Kojima, C., Minamino, T. *et al.* (2009). Stator assembly and activation mechanism of the flagellar motor by the periplasmic region of MotB. *Mol. Microbiol.* **73**, 710–718.
19. Song, H., Sandie, R., Wang, Y., Andrade-Navarro, M. A. & Niederweis, M. (2008). Identification of outer membrane proteins of *Mycobacterium tuberculosis*. *Tuberculosis (Edinb.)*, **88**, 526–544.
20. Grizot, S. & Buchanan, S. K. (2004). Structure of the OmpA-like domain of RmpM from *Neisseria meningitidis*. *Mol. Microbiol.* **51**, 1027–1037.
21. Parsons, L. M., Lin, F. & Orban, J. (2006). Peptidoglycan recognition by Pal, an outer membrane lipoprotein. *Biochemistry*, **45**, 2122–2128.
22. Delaglio, F., Grzesiek, S., Vuister, G. W., Zhu, G., Pfeifer, J. & Bax, A. (1995). NMRPipe: a multidimensional spectral processing system based on UNIX pipes. *J. Biomol. NMR*, **6**, 277–293.
23. Johnson, B. A. (2004). Using NMRView to visualize and analyze the NMR spectra of macromolecules. *Methods Mol. Biol.* **278**, 313–352.
24. Jeschke, G., Chechik, V., Ionita, P., Godt, A., Zimmermann, H., Banham, J. *et al.* (2006). DeerAnalysis2006—a comprehensive software package for analyzing pulsed ELDOR data. *Appl. Magn. Reson.* **30**, 473–498.
25. Shen, Y., Delaglio, F., Cornilescu, G. & Bax, A. (2009). TALOS+: a hybrid method for predicting protein backbone torsion angles from NMR chemical shifts. *J. Biomol. NMR*, **44**, 213–223.
26. Schwieters, C. D., Kuszewski, J. J., Tjandra, N. & Clore, G. M. (2003). The Xplor-NIH NMR molecular structure determination package. *J. Magn. Reson.* **160**, 65–73.
27. Laskowski, R. A., Rullmannn, J. A., MacArthur, M. W., Kaptein, R. & Thornton, J. M. (1996). AQUA and PROCHECK-NMR: programs for checking the quality of protein structures solved by NMR. *J. Biomol. NMR*, **8**, 477–486.